Changes in misorientations of grain boundaries in titanium during deformation

G. Salishchev[a], *S. Mironov*[b,c], *S. Zherebtsov*[a,*], *A. Belyakov*[d]

[a]*Laboratory of Bulk Nanostructured Materials, Belgorod State University, 85 Pobeda Str., Belgorod, 308015, Russia*
[b]*Department of Materials Processing, Graduate School of Engineering, Tohoku University, 6-6-02 Aramaki-aza-Aoba, Sendai 980-8579, Japan*
[c] *Institute for Metals Superplasticity Problems, Russian Academy of Science, 39 Khalturin Str., Ufa, 450001, Russia*
[d] *Laboratory of Mechanical Properties of Nanoscale Materials and Superalloys, Belgorod State University, 85 Pobeda Str., Belgorod, 308015, Russia*

A B S T R A C T

The changes in grain boundary misorientations during plastic deformation of titanium were studied by means of the EBSD technique. The misorientation of all types of the grain boundaries including low- and high-angle boundaries, coincident site lattice (twin) and arbitrary boundaries, deformation-induced boundaries and the boundaries of the original grains was found to change during deformation. It was shown that the deformation may result in either increasing or lowering of the boundaries misorientation and different segments of the same grain boundary may develop principally differently. The most significant changes of the boundary misorientation were found to be associated with the boundary junctions. The change in misorientations during deformation was discussed in terms of the interaction of a boundary with dislocations and/or with other boundaries.

Keywords:
Titanium
Plastic deformation
EBSD
Grain boundary
Change in misorientation

1. Introduction

Severe plastic deformation (SPD) has been recently utilised as a novel processing method for the production of bulk submicrocrystalline metallic materials. The process of microstructure refinement during large plastic deformation of metals and alloys is mainly associated with the development of deformation-induced boundaries (DIBs) [1,2]. This phenomenon can be briefly summarized as follows: (i) two different types of deformation-induced boundaries can be distinguished, ordinary cell boundaries (incidental dislocation boundaries, IDBs) arising from a statistical mutual trapping of dislocations, and geometrically necessary boundaries (GNBs) caused by different activities of slip systems across the boundary [3]; (ii) the misorientation angle of both GNBs and IDBs continuously increases during deformation. The GNBs may increase their misorientations up to typical values of ordinary grain boundaries, while the misorientations of IDBs saturate at a level of dislocation subboundaries [4]. It should be noted that this statement is based on statistically averaged data, i.e. boundary misorientations are discussed in terms of the mean misorientation angle and the fraction of high-angle boundaries (HABs) [3]; (iii) the change of misorientation angle of an IDB is related to storage of excess density of one-sign dislocations within a boundary. The Read–Shockley relation [5] is commonly used for description of this process: $\theta = b\, d\, \Delta\rho$, where θ is the misorientation angle of a dislocation boundary, b — the Burgers vector, d — a mean spacing between the dislocation boundaries and $\Delta\rho$ is the excess density of one-sign dislocations within the boundary.

The successful application of the SPD for the production of the ultrafine-grained materials does require a fundamental

* *Corresponding author.* Tel.: +7 4722 585 416; fax: +7 4722 585 415.
E-mail addresses: Zherebtsov@bsu.edu.ru, ser_z@mail.ru (S. Zherebtsov).

understanding of the key physical mechanisms governing the process of the grain boundary misorientation evolution. The typical approach which is currently used for this purpose involves the study of large datasets of grain boundaries to obtain statistically averaged data for deformation-induced behaviour of the grain boundaries. In this case, however, there is a chance that some important details of the behaviour of the individual boundaries can be missed. The authors show that the analysis of both (i) the evolution of the global misorientation distribution as well as (ii) the deformation behaviour of the individual boundaries is needed to describe an evolving microstructure adequately. In an attempt to provide a deeper insight into the grain boundary evolution during plastic working, the present paper focuses on the study of the misorientation changes of individual boundaries and their relationship with the deformation-induced subboundaries.

2. Experimental

Commercial-purity titanium of Grade 2-type (0.07Fe, 0.05C, 0.012H, 0.09N, 0.1O, all in wt.%) was used as the experimental material. This metal has a comparatively simple behaviour that is relatively well documented. The material was received as a hot-rolled bar with a homogeneous recrystallized grain structure and an average grain size of 20 μm. A prismatic sample of $14\times16\times20\ mm^3$ was machined parallel to the bar axis and compressed to 40% of height reduction at 400 °C and at an initial strain rate of 10^{-3} using a Schenk universal testing machine. These deformation conditions were found to be optimal for microstructure refinement, i.e. DIBs development, in titanium during SPD [6].

For structural investigations, the deformed sample was sectioned perpendicular to the compression axis at approximately a quarter of its height. The examined surface was located in the middle between severely deformed central area and almost unstrained peripheral face. In this case an optimal accuracy and representativeness of the EBSD analysis may be expected. The obtained specimen was ground and finally electro-polished in a solution of 20% perchloric acid in acetic anhydride at a temperature of 10–20 °C with an applied potential of 60 V. To allow a direct comparison with initial (undeformed) microstructure, a thin slice was cut from the supplied hot-rolled bar normal to the bar axis and was polished in a similar fashion.

The polished specimens were analysed by using the electron back-scatter diffraction (EBSD) technique. An INCA Crystal™ EBSD system interfaced to a JSM-840A W-filament scanning electron microscope (SEM) was employed for this purpose. Orientation mapping involving automatic beam scanning was used with a scan step size of 0.1 μm and the EBSD maps of ~50,000 pixels typically encompassing several original grains were obtained. The pattern solving efficiency was ~95% and 80% for initial and deformed materials, respectively. The non-indexed data points were automatically reassigned to the crystallographic orientations belonging to their nearest neighbours in order to obtain a higher fidelity picture of the grain boundary regions and thus a more accurate determination of the misorientation across the boundaries. In EBSD maps presented in this paper, black and grey lines indicate high- and low-angle boundaries, respectively, and a 15° criterion was used to define low-angle versus high-angle boundaries. Since the experimental accuracy for orientation evaluation by the EBSD method commonly does not exceed 1° [7], the grain boundaries below 2° were excluded from the consideration.

The EBSD technique involved automatic orientation mapping on a grid with the step of 0.1 μm in our case, and thus it enabled misorientation measurements in many points along the same boundary. This provided a possibility to evaluate misorientation along a boundary and in the vicinity of triple junctions. The maximum distance from a boundary or triple junctions to the point of measurement did not exceed 100 nm (scan step), and the mean value of the distance might be around 50 nm. Taking into account a diameter of the electron beam which is approximately 10–20 nm, the mean relevant distance was even smaller: about few tens of nanometer.

The change of misorientation along a boundary was estimated as a relative increase or decrease of misorientation of each next part with respect to the previous point of measurement. Also a difference between the minimum and maximum absolute values of misorientation along the same boundary was estimated.

3. Results

An EBSD map of the initial (undeformed) titanium is shown in Fig. 1; misorientation of some boundaries is indicated in degrees. It is clear that the HABs are arranged into a continuous network following the original grains while the low-angle boundaries (LABs) are clustered within some grains.

In the undeformed condition (Fig. 1), the misorientation angle does not change along the majority of the original grain boundaries. However in two cases indicated with arrows the variation of the boundary misorientation was found to be about 2°. Therefore, the misorientation angle of these boundaries is *variable* along their lengths. It is notable that the variations of the misorientations of HABs were observed at those points were LABs join the HABs (Fig. 1).

A typical EBSD map of the deformed microstructure is shown in Fig. 2a and magnified images of two selected regions are given in Fig. 2b and c. The plastic deformation significantly complicates the structure morphology by introducing an abundance of the LABs; additionally, HABs and twins are occasionally observed in grain interiors. Nevertheless, the original grain boundaries are still clearly recognizable. EBSD measurements revealed that the misorientation angle appreciably varies along grain boundaries in the deformed microstructure.

A magnified image of a typical original grain boundary region is shown in Fig. 2b; misorientations of some boundaries are indicated in degree. The original grain boundaries as well as the deformation induced HABs and LABs in the grain interior clearly exhibit the local changes of the misorientation angle along boundaries. Frequently, the level of the local misorientation changes is very close to the detectable limit

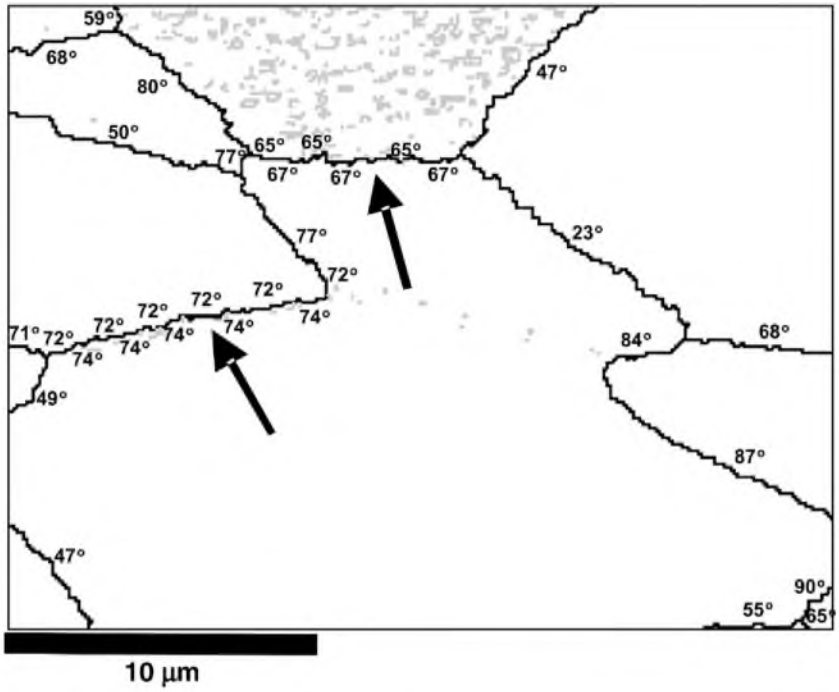

Fig. 1 – Typical EBSD map of initial (undeformed) microstructure. The local misorientation of some boundaries is indicated in degrees. High-angle boundaries are indicated in black, and low-angle boundaries are in grey.

(~2°); in some cases, however, their magnitude reaches up to 12° (arrowed in Fig. 2b).

In general, the deformed microstructure displays a much higher level of the misorientation changes along boundaries than that in the initial material (Fig. 1). This implies that the plastic deformation introduces the misorientation changes into the grain boundary structure. The pattern of the local misorientation change is generally complex and the misorientation angle usually varies in an erratic way, exhibiting either periodic behaviour or cumulatively increasing (or decreasing) along a boundary. For example, the misorientation angle changes along an original grain boundary from 34° to 52° (Fig. 2b).

In order to gain a better understanding of this process, the variations of the misorientation angle along twin boundaries have been studied. As the twin boundaries satisfy an a priori known misorientation relationship, twins can serve as an ideal tool in the analysis of the local misorientation changes. A magnified view of a typical twin is given in Fig. 2c; misorientation of some boundaries is indicated in degree. The misorientation between the twinned region and the matrix is close to a Σ13b boundary (57.42° rotation about $<2\bar{1}\bar{1}0>$). This specified misorientation relationship indicates that the active twin family is most likely to be $\{10\bar{1}1\}$ compressive twins. In the previous investigation [6] the predominance of this twin mode has been confirmed statistically from the misorientation distribution, which shows a high fraction near the misorientation angle of 60° and the misorientation axis of $<2\bar{1}\bar{1}0>$.

According to [8] the maximum permissible deviation from a perfect twin coincidence (Brandon's tolerance) may be calculated as $\Delta\theta = 15^{\circ} / \sqrt{\Sigma}$ that for a Σ13b boundary equals 4.1°. In the present case, EBSD measurements revealed that the perfect twin-matrix misorientation of 57.42° e.g. [6] was destroyed due to the presence of the misorientation changes along the twin boundary. Though the local misorientation changes were typically close to the noise level (≈±2°), they do show a significant angular deviation of the measured misorientation from the perfect twin relationship; locally, the misorientation increases up to 64° or it decreases down to 52°. It is an interesting observation that the 'special' boundary of the twin becomes random in character locally as its deviation from the exact twin misorientation exceeds the Brandon's tolerance. Two principal observations can be made from this figure. Firstly, plastic deformation may result in the lowering of the boundary misorientations. This observation is of particular interest because severe plastic deformation is usually associated with the continuous increase of the misorientation angle of the DIBs e.g. [2,4,9,10]. However, the microstructural evidences in this study indicate that this process is only a global trend but not an indispensable principle for each particular boundary. Secondly, different segments of the same boundary may evolve differently — towards increasing as well as decreasing the misorientation. By generalizing these findings, it can therefore be concluded that misorientation of a particular boundary may develop arbitrarily (i.e. both increase and decrease are possible) and heterogeneously (different segments of the same boundary may evolve differently).

In an attempt to enable a statistical view on the deformed condition, a total of 357 changes in misorientation found along the boundaries of different boundary types (the original grain boundaries, twin boundaries, LABs and HABs in grain interiors) were analysed in the present study. The size

distribution of the local misorientation changes is shown in Fig. 3a. All data points fall on the same master curve exhibiting an abundance of the minimal detectable change in misorientation (±2°) that drops off quickly with the increasing of the variation magnitude. It should be stressed however that the 2° misorientation changes are very close to the noise level and thus it is difficult to be sure whether they are real or not. The angular spread of the misorientation changes is large with the maximum reaching up to 18° (Fig. 3a).

Frequently, the local misorientation changes were observed at triple junctions, which were typically formed by the intersecting LABs and HABs. To examine the effect of the boundary intersections, the percentage of the misorientation

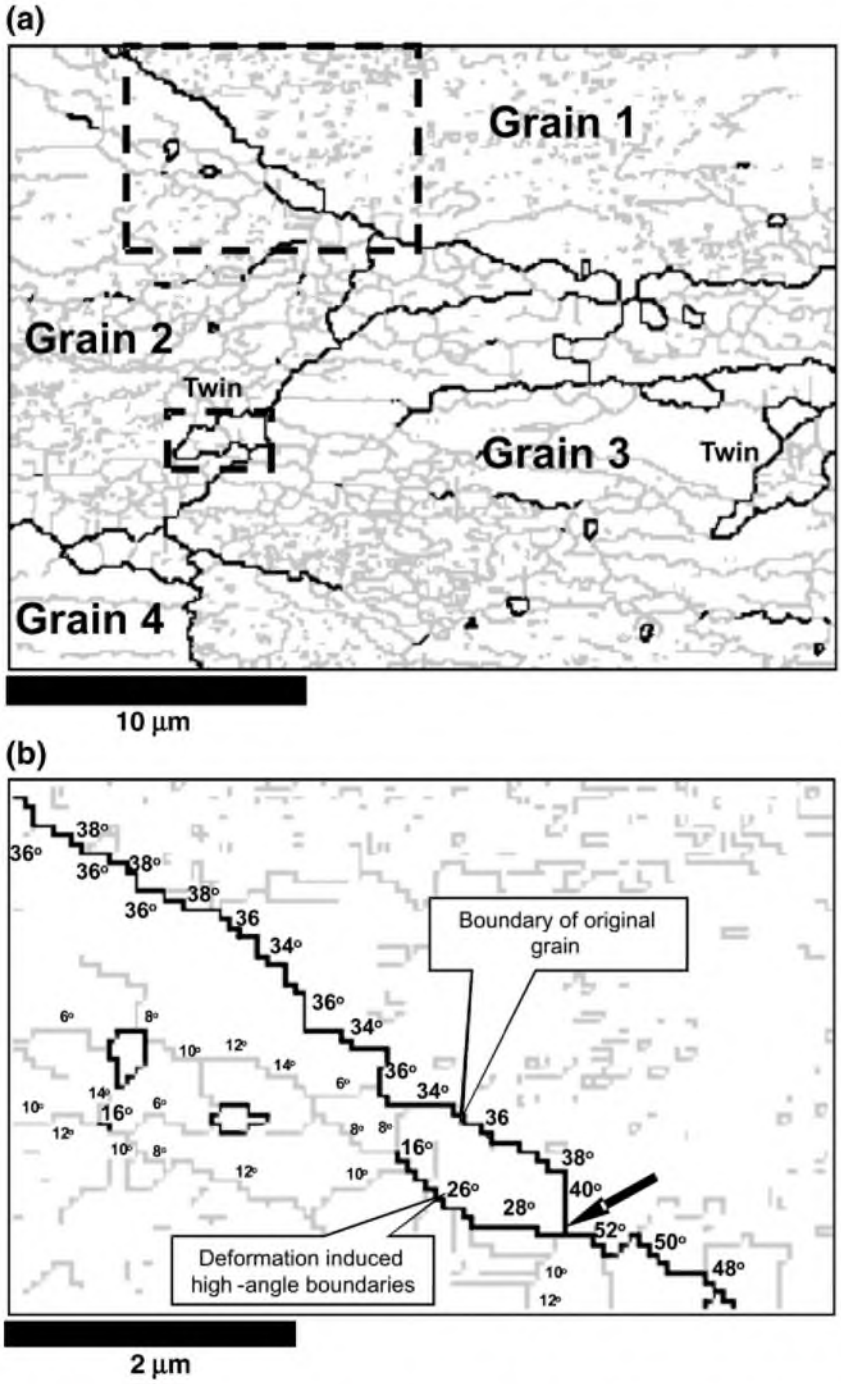

Fig. 2 – Typical EBSD map showing local boundary misorientation angles in the deformed microstructure (a) and magnified images of selected regions: region of the original grain boundary (b) and twin (c). High-angle boundaries are indicated in black, and low-angle boundaries are in grey.

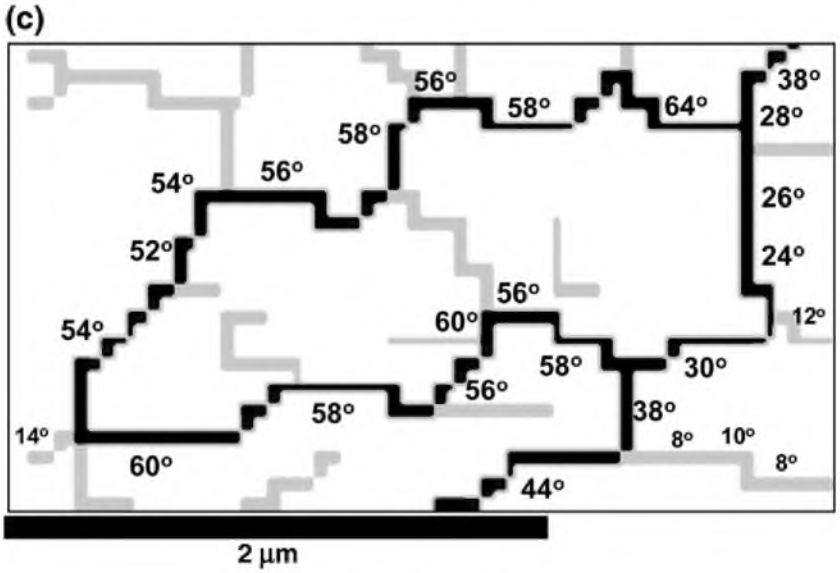

Fig. 2 (*continued*).

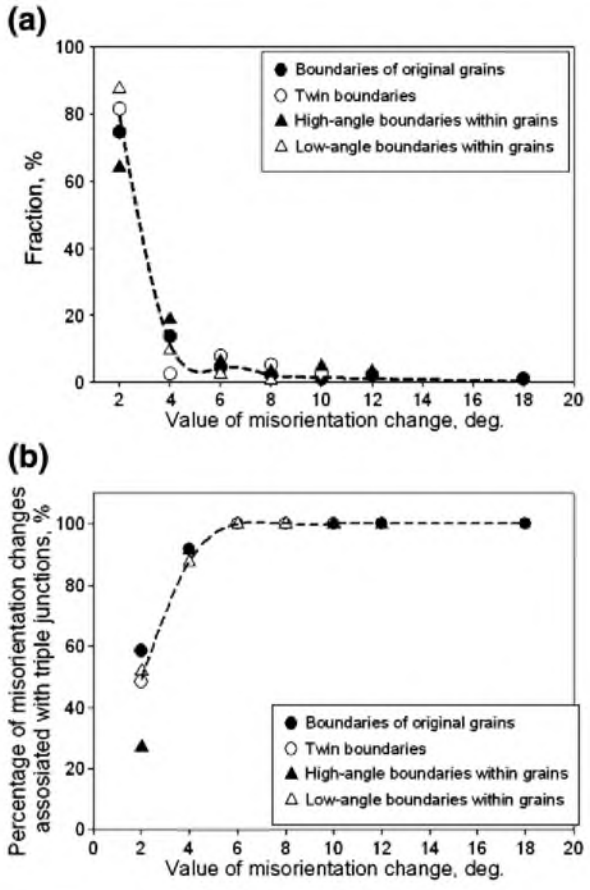

Fig. 3 – Distributions of misorientation changes (a) and effect of boundary intersections (b) on the value of misorientation changes. The change of misorientation was estimated as a relative increase or decrease of misorientation of each next part of the boundary with respect to the previous point of measurement.

changes associated with the triple junctions was plotted against the size of the local misorientation change, as shown in Fig. 3b. Again, all data points corresponding to the different boundary categories fall closely together illustrating the same general behaviour. The graph indicates that the proportion of the misorientation changes associated with the triple junctions increases rapidly in the range of 2–4° and reaches 100% at 6° (Fig. 3b). Therefore, all local misorientation changes in excess of 6° were associated with the triple junctions.

4. Discussion

The detailed inspection of the deformation behaviour of the individual boundaries shown in the previous section has revealed that the misorientation across all types of the grain boundaries (including the original grain boundaries, twin boundaries LABs and HABs of the deformation origin) changes during strain. These changes are not associated solely with the increase of the misorientation but the deformation may also result in the lowering of the boundary misorientation.

Different segments of the same grain boundary may evolve principally differently — towards increasing or decreasing of the misorientation. The observed changes in misorientation along grain boundaries evidently indicate the heterogeneous nature of deformation. Of particular interest is the finding that the most significant changes of the boundary misorientations are associated with the boundary junctions, as shown in Fig. 3b.

As mentioned above, the change in the misorientation angle of a DIB during deformation is usually attributed to the accumulation of one-sign dislocations by the boundary. Obviously, this mechanism (described by the Read–Shockley relation) must lead to a uniform and gradual increase in the boundary misorientation. However, the Read–Shockley relation cannot explain the variation of misorientation change along a

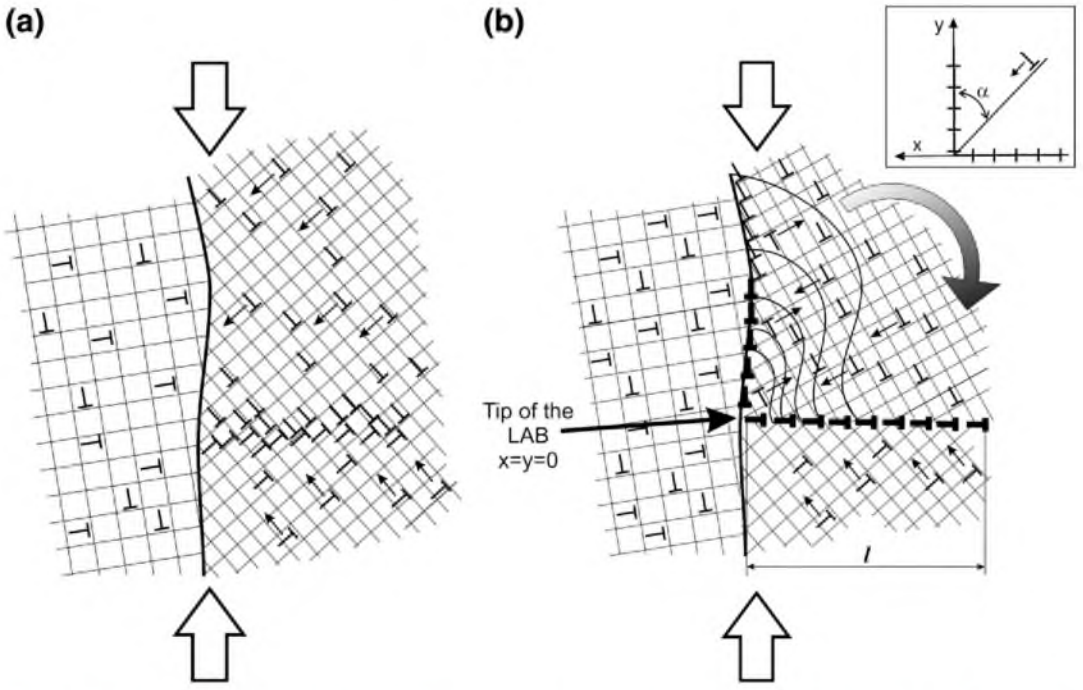

Fig. 4 – Schematic drawing for evolution of the dislocation array (a) and low-angle boundary (b) near the initial grain boundary during deformation. In (b) the distribution of shear stresses in the right top (sub)grain in the vicinity of the LAB tip is schematically shown by lines of equal stresses. The inset in (b) shows the coordinate system used. Compression direction is shown by arrows.

boundary. The local change in a boundary misorientation can be caused by the local development of secondary slip, which can occur at boundary junctions. A simplified model explaining local misorientation changes of grain boundaries during deformation is described below.

Multiple slip (which is typical near original grain boundaries) usually results in the formation of a dislocation array near a boundary, as schematically shown in Fig. 4a. Upon further straining, the dislocation array may transform into an incomplete dense dislocation wall and then into a LAB joined to the original grain boundary (Fig. 4b). For the sake of simplicity the array of dislocations that comes from various slip systems and composes the LAB is shown as a wall of "thick" dislocations in Fig. 4b. The point of the joint between the LAB (tip of the LAB) and the original grain boundary has the coordinates $x=y=0$. The employed coordinate system is shown in the top right corner of Fig. 4b: the y-axis is directed along the original grain boundary, the x-axis is directed along the LAB. The newly developed LAB with the length of l may be described in terms of the Burgers vectors of the constituent dislocations, b, and the spaces between dislocations, D. The compressive normal stress in the vicinity of the LAB tip may be evaluated as follows [11]:

$$\sigma_{xx} = -\frac{\mu b}{2\pi(1-\nu)D}\left[\frac{x^2}{x^2+y^2} - \frac{x^2}{x^2+(y+l)^2} + \frac{1}{2}\ln\frac{x^2+(y+l)^2}{x^2+y^2}\right] \quad (1)$$

where μ — is the shear modulus; ν — is the Poisson's ratio and x and y are the coordinates. The maximum stress arises around the tip of the LAB. This stress influences the initial HAB with the magnitude of the shear stress $\tau=\sigma_{xx}\cos\alpha$, where α is the angle between the y-axis and the slip plane with the maximum Schmidt factor. Taking the value of $\alpha=45°$, the shear stress, $\tau=0.707\sigma_{xx}$. The distribution of shear stresses calculated using Eq. (1) in the vicinity of the LAB tip is schematically shown in Fig. 4b by lines of equal stresses (curved thin solid lines). Note here, that the neighboring (sub)grain experiences the same (symmetric) stress distribution.

The level of stresses affecting an initial HAB after the formation of a LAB in titanium can be evaluated as follows: the ratio of b/D is linked with misorientation of the LAB; a

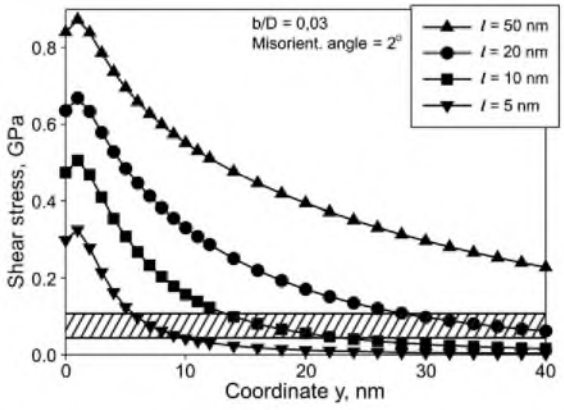

Fig. 5 – Relationships between the level of the shear stress and the distance from the dislocation boundary (y) for various boundary lengths (l) (see Fig. 5). The level of stresses required for dislocations emission by an arbitrary HAB in various materials is indicated by the shadowed area.

frequently observed misorientation angle of $\omega = 2°$ for deformation induced incomplete dislocation boundaries (LABs) results from the ratio of $b/D = \mathrm{tg}(\omega) = 0.03$. Taking the values of $\mu = 43.5$ GPa and $\nu = 0.32$, a set of shear stresses as function of coordinate y (distance from the junction point) for various lengths l of the LAB can be obtained (Fig. 5). It is seen, that the stresses along the initial boundary decrease fast with increasing y. According to [12] the stress required for dislocations emission by an arbitrary HAB in various materials falls in the interval from $\mu/1000$ to $\mu/400$ (shadowed area in Fig. 5). It is seen from Fig. 5 that the stresses, induced by the LAB, are high enough to initiate the dislocation emission from part of the HAB in the vicinity of the LAB. Certainly, both the stress and the distance where the local stress exceeds the threshold of dislocation emission, increase with the increase of misorientation of LAB. The development of secondary slip that is caused by the formation of LAB results in a local change in the misorientation of a portion of pre-existing HABs. Therefore, the process of boundary misorientations changing during deformation is by superposition of the accumulation of lattice dislocations and the emission of secondary dislocations by a grain boundary. Similarly, the development of secondary slip leads to the local change in boundary misorientations at any HAB junction. The dislocation fluxes that are caused by plastic deformation result in the accumulation of excess boundary dislocations. These excess boundary dislocations act on portions of HABs as the low-angle dislocation boundary in Fig. 4 and can initiate the emission of secondary dislocations.

Once the low-angle DIB has developed, its misorientation continuously increases accompanied by a gradual rotation of adjacent grains upon further deformation. Such DIB can be considered as geometrically necessary boundaries resulting from incompatibilities of strain in adjacent grains [4]; and their misorientations can enlarge to the high-angle range. As the process proceeds the DIB in turn becomes a source for another low-angle boundary. Indeed, our results show that all deformation-induced HABs are 'branched', i.e. they are always in contact with at least one LAB (Fig. 3). From the analysis above the development of new dislocation boundaries initiates high local stresses that stimulate local secondary slip at boundary junctions.

Therefore interaction with newly developing low-angle dislocation boundaries is one of the significant factors changing the misorientation of the HAB, although some change in the misorientation along a boundary may also be caused by heterogeneity in the dislocation flux through a given grain because of different orientations of most highly activated slip systems in neighboring grains. It can be concluded that the interaction between slip process and grain boundaries affects the formation of HABs and, hence, structure refinement during SPD. The misorientation of any type of boundaries ("new" deformation-induced and "old" boundaries of initial grains, low- and high-angle, coincident site lattice and arbitrary) can be changed by this way.

The misorientation of a boundary is described by both misorientation angle and rotation axis. That is why a change in the misorientation cannot be calculated by simple summation/deduction of misorientations of involving boundaries. Junctions of boundaries with the same misorientation angle can cause different changes in misorientation angle of contacting boundaries that depends on the features of local dislocation processes. Therefore the misorientation changes occurring in the vicinity of the junction points may be differently directed (towards either increasing or decreasing of the misorientation) and unequal (different segments of the same boundary can have different misorientations). Such interactions of boundaries with each other during SPD can be a reason for the development of misorientation distributions which are close to random (e.g. [6,13]).

5. Conclusions

The EBSD technique has been employed to study the deformation behaviour of individual grain boundaries during plastic deformation. Two conclusions were made from the present work.

1) The misorientation across all types of the boundaries (original and deformation-induced), coincident site lattice (twin) and arbitrary boundaries, low- and high-angle boundaries, changes during deformation. The deformation may result in increasing as well as lowering of the boundaries misorientation. Different segments of the same boundary may evolve differently — towards either increasing or decreasing of the misorientation.
2) The formation of the deformation-induced boundaries adjoined to an original grain boundary was shown to enhance the mutual crystallographic rotation of the adjoined grains and thus cause local misorientation changes that vary spatially across the original grain boundary.

Acknowledgements

This work was supported by Federal Agency for Science and Innovations, Russia, under Grant No. 02.740.11.0119.

REFERENCES

[1] Rybin VV. Large plastic deformation and fracture of metals. Moscow: Metallurgia; 1986.
[2] Humphreys FJ, Prangnell PB, Bowen JR, Gholinia A, Harris C. Developing stable fine-grain microstructures by large strain deformation. Phil Trans R Soc Lond 1999;A357:1663–81.
[3] Hansen N, Jensen DJ. Development of microstructure in FCC metals during cold work. Phil Trans R Soc Lond 1999;A357: 1447–69.
[4] Kuhlmann-Wilsdorf D, Hansen N. Geometrically necessary, incidental and subgrain boundaries. Scr Metall Mater 1991;25: 1557–62.
[5] Read WT, Shockley W. Dislocation models of crystal grain boundaries. Phys Rev 1950;78:275–989.
[6] Mironov SYu, Salishchev GA, Myshlyaev MM, Pippan R. Evolution of misorientation distribution during warm '*abc*' forging of commercial-purity titanium. Mater Sci Eng 2006; A418:257–67.
[7] Humphreys FJ. Quantitative metallography by electron backscattered diffraction. J Microsc 1999;195:170–85.

[8] Brandon DG. The structure of high-angle grain boundaries. Acta Metall 1966;14:1479–84.
[9] Davis RK, Randle V. Orientation perturbations near triple junctions in a non-cell forming aluminium–magnesium alloy. Mater Sci Eng 2000;A283:251–65.
[10] Nesterova EV, Rybin VV. Mechanical twinning and fragmentation of commercially pure titanium at the stage of advanced plastic deformation. Ph Met Metallogr 1985;59: 395–406 (in Rusian).
[11] Hirth JP, Lothe J. Theory of dislocationssecond ed. New York: Wiley; 1982.
[12] Kurzydlowski KJ, Varin AR, Zielinski W. *In situ* investigation of the early stages of plastic deformation in an austenitic stainless steel. Acta Metall 1984;32:71–8.
[13] Gholinia A, Prangnell PB, Markushev MV. The effect of strain path on the development of deformation structures in severely deformed aluminium alloys processed by ECAE. Acta Mater 2000;48:1115–30.